ISBN: 978-3-95450-240-0 ISSN: 2673-5547 doi:10.18429/JACoW-HIAT2022-MO1C3

HIGH VOLTAGE UPGRADE OF THE 14UD TANDEM ACCELERATOR

T. B. Tunningley, S. T. Battisson, A.C. Cooper, J. Heighway, H. D. Hinde, C. Kafer, T. Kitchen, N.R. Lobanov, P. Linardakis, C. Notthoff†, B. Tranter, D. Tempra, and R. Tranter
Heavy Ion Accelerator Facility, Australian National University, Canberra, ACT, Australia
R.A. Bosch, J.E. Raatz, National Electrostatics Corp. Middleton, WI, USA

Abstract

The 14UD at the Australian National University's Heavy Ion Accelerator Facility (HIAF) operated at a maximum voltage of 15.5 MV after the installation of tubes with a compressed geometry in the 1990s. In recent years, the performance of the accelerator has shown a gradual decline to a maximum operation voltage of ~14.5 MV. There are some fundamental factors that limit the high voltage performance, such as SF6 gas pressure, field enhancement due to triple junctions and total voltage effect. In addition, there are non-fundamental factors causing high voltage degradation. These are: operation with faulty ceramic gaps; operation at inappropriate voltage and SF6 pressure combinations; SF6 leaks into the vacuum space; use of SF6 and O2 as a stripper gases; poor electron suppression in the high energy stripper and frequent use of highly reactive ions such as sulphur and fluorine. In 2019 ANU initiated a feasibility study of available options to upgrade the entire population of supporting posts, acceleration tubes and grading resistors. In this paper we will discuss the preferred technologies and strategies for successful implementation of this development. The chosen design is based on NEC tubes with magnetic electron suppression and minimized steering of ion beams.

INTRODUCTION

Accelerator users are most familiar with tubes that are the products of three commercial suppliers: NEC, HVEC and Dowlish. Each manufacturer features a particular type of electron suppression technology.

The original NEC 333 kV tubes were assembled with "dead" sections of the lowest longitudinal field containing a substantial radial component to suppress the multiplication of particles that originated on electrodes. In the later compressed geometry, "dead" sections were removed and in order to restore strong axial field modulation, the electrodes were of variable diameter and dished [1, 2]. In Munich, the 25 mm thick, 25 mm diameter heater plate was replaced by a "zero" length 25 mm diameter electrode resulting in inferior trapping efficiency for ions and electrons originating from the aperture and from ionization of residual gas. To improve the trapping, V-shaped electrodes with angles ranging from 30 up to 50 degrees were successfully introduced to replace the flat electrode.

Still, no suppression existed for gas ionizations near the axis. In the 1990s, the overall length of a single tube increased to allow for operation up to 500 kV. Each section contained 21 live gaps with V-electrodes every 10 or 11 gaps. The trapping efficiency of Vs installed in the middle of tubes was weaker. In later tube designs, the V-electrodes were removed completely and weak magnets added to provide suppression of particles that originated on apertures and in gas [3]. The transverse magnetic field rotates by 90 degrees after every ~7 gaps of the tube.

However, this scheme was not optimum. After the New Delhi machine, NEC changed the tubes to use two pieces per MV, with either 20 or 21 ceramic gaps depending on the accelerator modules. NEC has used 20 and 21 gap tubes with 50 degree cones without external magnets in at least 7 accelerators, including the 20UR at JAEA-Tokai. This solution works even though the lack of suppression may limit heavy-ion beam currents.

At the same time, NEC has used similar tubes with 22 gaps but without cones in tandems up to 6 MV, and they conditioned very well. Again, the lack of suppression may limit heavy-ion beam currents. Based on these results, NEC has made a short-term decision to add weak magnets to the 22 gap tubes for 6 MV systems. In this module, there are 4 apertures per 1 MV, without cones, with 1 aperture in the middle on each 22 gap tube, that is, 11/11. The magnetic field reaches 47 gauss on axis between apertures and falls off near each aperture because the field is rotated 90 degrees from one set of 11 gaps to the next. In the 6 MV case, the modelling shows an average electron energy of only 222 keV and, with just 6 MV of length, an easily correctable net deflection for protons. These new tubes all have one internal 1 inch aperture, so for the modules of the 14UD there would be four 10-gap intervals between apertures per MV. NEC does not use cones in any apertures. These tubes have been used in all "U-series" accelerators since New Delhi and, at least up to 6MV and 8MV, NEC finds them to be well behaved. The U-series use the ceramic posts as in the 14UD, as opposed to smaller S-series, which uses an acrylic column. Magnets are external, hidden in the spark gaps.

The focus of this study is to evaluate suppression efficiency for charged particles originating on axis and on the surfaces of Ti electrodes. Suppression devices should not compromise the transmission of the ion beam, both CW, pulsed, chopped and bounced (AMS) in the full ranges of accelerating voltages from a few MV up to 14.5 MV and mass range from M=1 (protons) up to M=244 (Pu).

The goal of this study to select an appropriate tube technology which will deliver at least the same performance of the 14UD accelerator or exceed it in terms of transmission, e-suppression and improved beam loading. This will be strongly dependent on simulations as the practical confirmation is mainly demonstrated in 6 MV machines, which are much smaller than the 14UD.

† email address: Christian.notthoff@anu.edu.au

ISBN: 978-3-95450-240-0 ISSN: 2673-5547 doi:10.18429/JACoW-HIAT2022-MO1C3

METHODS

Experimental Evidence of Secondary Particles Generated Inside Accelerating Tubes

Experience with the 14UD tandem at ANU has shown that the interaction of the heavy ion beam with the residual gas atoms in the tube and bombardment of Ti apertures and electrodes can lead to critical limitations of the transmitted beam intensity due to beam loading and vacuum problems. Five acceleration tubes were replaced with viable used spares during a maintenance period in 2016. Three eleven-gap tubes above the high-energy stripper were removed from unit 19 and two eleven-gap tubes were removed from below the stripper in unit 20. The titanium insert electrodes within the tubes were removed and examined using an optical microscope [4].

SIMION Simulations of e-Supression, Steering and Effect on Spread of Pulse Width

The model was constructed using a bitmap (created from an Inventor model cross section) to PA conversion in Simion SL Tools. Then it was converted to an axisymmetric array and voltages were assigned at graduations of 30kV giving a range of 0 V-990 kV across the three tubes.

To simulate the electron suppression, two groups of electrons were considered. In the first group, electrons originated on the beam side of the V electrode. The second group comprised of the electrons originated near the axis from interactions with the residual gas.

Being on or near the axis, the blue trajectories are difficult to stop and accelerate up towards the terminal.

Analytical Simulaaations of the Effect of Magnetic Steering Applied to the Entire LE or HE Sections of the Accelerator

Some limitations of the SIMION package would not allow a model of the full machine. However, a simple analytical model can be derived from the Lorentz equation in order to estimate beam deflection by magnets applied to the entire LE or HE sections of the 14UD. In the case of high gradient tubes with magnets, the typical tube section geometry is divided into 4 segments of length l_1, l_2, l_3 and l_4 in which the magnetic field is rotated by 90° from one segment to another. In segment 1, the magnetic field **B** is applied towards the reader therefore the beam is deflected and exits this segment at angle θ_1. In segment 2, the trajectory is nearly a straight line (in reality a parabola) as the ion is still accelerated due to **E** but no action from **B** in this projection. In segment 3, the ion is bent in the reverse direction as the magnetic field **B** is the opposite polarity as compared to segment 1. In segment 4, the ion travels nearly parallel to the axis but at slightly divergent angle as the velocity is higher than in segment 1. Segments 1 to 4 describe the full pattern of motion and then repeats further down in acceleration.

The analytical solution is based on the following assumptions.

1. The magnetic field suddenly changes direction by 90 degrees between sections.
2. The velocity of the particle within the section is assumed to be constant and defined as $\beta = (\beta_{in} + \beta_{out})/2$, where β_{in} is the velocity at the entry point and β_{out} is the exit velocity.
3. The "constant velocity approximation" assumes there is no electric field in sections 1 and 3 so the particle follows a circular path.
4. We assume that the deflection in section 1 is cancelled by the opposite deflection in section 3.The trajectory in section 4 is parallel to the axis.

Because of many assumptions, the analytical model will be validated by comparing with SIMION simulations for a short section of the accelerator. The deflection of particles after passing through the consecutive sections of the tube is given by a set of equations where the index corresponds to the number of segment

$$D_1 \approx 0.16 \times Q l_1^2 B/M\beta_1 \quad (1)$$

$$D_2 \approx l_2 \times \theta_1 = 0.32 \text{ x } QBl_1l_2/M\beta_2 \quad (2)$$

$$D_3 \approx 0.16 \times Q l_3^2 B/M\beta_3 \quad (3)$$

$$D_4 \approx 0, \quad (4)$$

where Q is the charge state, M is the atomic mass, β=v/c is the particle velocity and c is the velocity of light in a vacuum. The total displacement of a particle after passing all four sections is given by the equation

$$D_{1\text{-}4} \approx D_1 + D_2 + D_3 + D_4 \quad (5)$$

Alternative Magnet Positioning and Orientation to Reduce Overall Beam Steering

Alternatively, there is an option where the positioning of magnets is optimised to cancel out any net beam steering. Just to check this concept, this study also explores a configuration "snake".

RESULTS

Optical Investigation of Ti Electrodes

Figure 1 shows the image of the 1st (A) and 12th (B) Ti electrode removed from tube 1 in unit 19 of HE section.

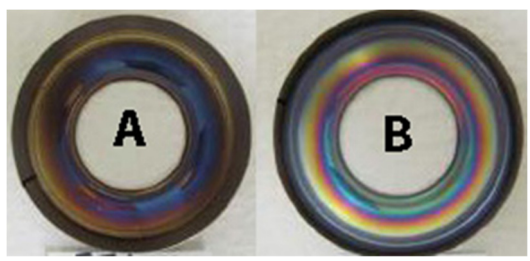

Figure 1: The image of the 1st (A) and 12th (B) Ti electrode removed from tube 1 in unit 19 after ~40 years of operation. Left image (A) is the discoloured electrode surface facing the top of accelerator and (B) is the surface of the 12th tube electrode facing the bottom of accelerator.

ISBN: 978-3-95450-240-0 ISSN: 2673-5547 doi:10.18429/JACoW-HIAT2022-MO1C3

SIMION Calculation of Secondary e⁻ Trajectories

Figure 2 depicts the result of SIMION simulations of the trajectories of secondary electrons in ANU's existing tubes with V electrodes and without magnetic suppression. Blue trajectories were added to simulate electrons liberated from interactions with the residual gas.

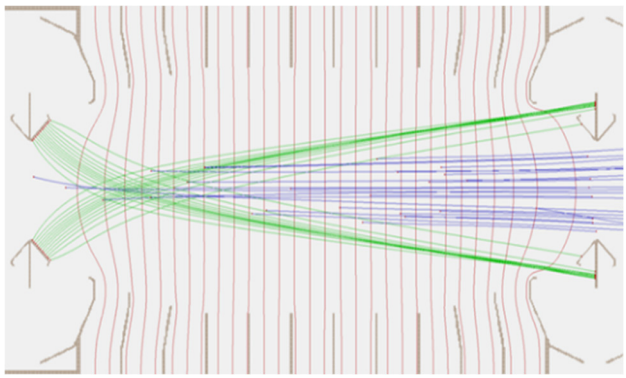

Figure 2: Electrons flying normal from Vee electrode (green) plus beam axis interactions (blue trajectories). No magnetic suppression.

Magnetic Suppression of Electrons Originating from the Aperture and from Ionization of Residual Gas

Table 1 lists the consolidated results of the simulation runs showing the percent of back-streaming electrons originating from the aperture through each section. Each section is 10 gaps defined by a 1" electrode, flat or V style. The higher the percentage, the more electrons through which is considered as negative effect. The magnets create 50 G field rotated by 90 degrees after every 7 gaps indicated as the spiral B field. The tube is the NEC 21 gap assembly.

Figure 3 shows the combined on-axis and aperture electron suppression on the 22-gap tube with both magnets and V electrodes.

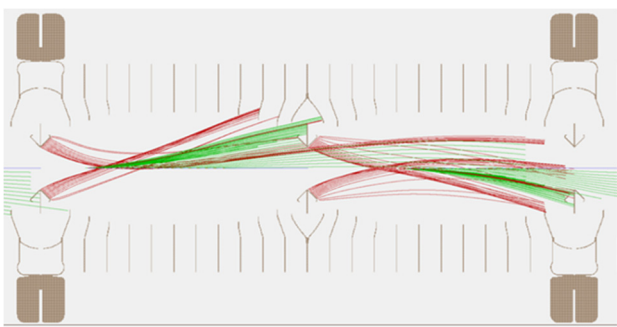

Figure 3: Electron suppression in XZ when both V electrodes and magnets are used.

The average energy at electron impact is 257 keV. For the Vee electrode generated electrons the average energy at impact is 286 keV (321 keV with no magnets).

Table 1: The percent of back-streaming electrons originating from the aperture through each section of a 21 gap high gradient tube.

Aperture	1	2	3	B-field
Flat at tube flange	100	30	0	none
Flat at tube middle	100	100	100	none
Flat with magnets XZ flange	0	0	0	spiral
Flat with magnets XZ middle	0	0	0	spiral
Flat with magnets YZ flange	15	0	0	spiral
Flat with magnets YZ middle	0	0	0	spiral
V electrode at tube flange	8	0	0	none
Flat at tube middle	100	100	100	none
V at tube flange	8	0	0	none
V at tube middle	36	9	0	none

Effect on Steering of the Ion Beam and Transmission by SIMION

In this section we will look at what effect the electron suppression magnets have on the beam steering. The tube is a 22 gap system with V electrodes and magnets rotating 90 degrees every 7 gaps. Two beams will be tested with SIMION, Proton (M=1) shown in red and Nickel (M=58) shown in green. The beams have an initial energy of 150keV and measurements are taken between magnet polarity changes. The gradient is 25kV per gap (1.97 MV/m). The overall effect is the beam steering off-axis as shown in Fig. 4.

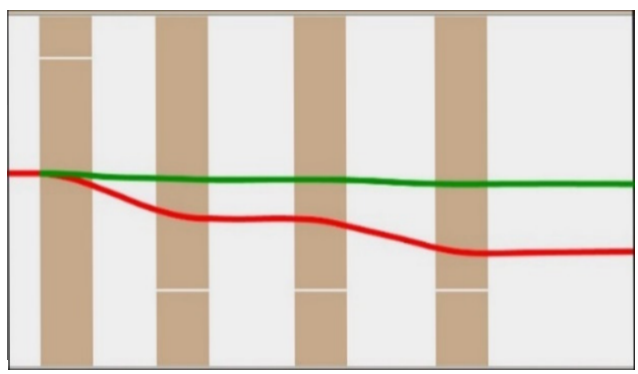

Figure 4: H^{-1} (red) and Ni^{-1} (green) beams in XZ plane stretched in the vertical axis to amplify trajectories. Each section (brown then white) indicates seven gaps and therefore the magnet orientations changing.

The beam displacement simulated with SIMION and by analytical formula is shown in Table 2.

ISBN: 978-3-95450-240-0 ISSN: 2673-5547 doi:10.18429/JACoW-HIAT2022-MO1C3

Table 2: Beam Displacement After Passing Through Three 22 Gap Tubes with Magnets

	LE section				HE section	
	H^{-1} D, mm		Ni^{-1} D, mm		Ni^{+12} D, mm	
X	SIMION	(7)	SIMION	(7)	SIMION	(7)
T1 in	0	0.0	0	0.0	0	0.0
T2 in	0.9	1.0	0.11	0.1	0.3	0.3
T3 in	1.4	1.4	0.18	0.2	0.6	0.4
T3 out	1.8	1.8	0.23	0.2	0.9	0.5

The beam displacement due to the effect of magnets after travelling through the entire LE and HE sections of the 14UD accelerator calculated with the analytical formula is shown in Table 3.

Table 3: Beam displacements at the end of LE and HE sections of 14 UD calculated with the analytical formula.

			LE section			HE section		
	E_{inj}, MV	U_T, MV	M	Q	D, mm	M	Q	D, mm
H	0.1	14.5	1	1	6.0	1	1	3.2
H	0.1	3	1	1	14.0	1	1	7.0
C	0.15	14.5	12	1	2.0	12	5	3.2
C	0.15	6	12	1	2.9	12	5	5.0
Cl	0.15	14	37	1	1.1	37	7	2.3
Cl	0.15	10	37	1	1.3	37	7	2.8
Ni	0.15	14.5	60	1	0.9	60	12	2.6
Au	0.15	14	197	1	0.5	197	13	1.5

Effect on Pulsing Width

The magnetic field causes deviations in path length of particles starting at different radii. The transit time changes as $\Delta t/t = \Delta L/L$. In the case of the pelletron accelerator, the major contributor to transit time is the first section of the accelerating column, the remaining sections add only a small fraction of the transit time broadening. The SIMION simulated transit time variations are given in Table 4.

In Table 4, the Δt is the time difference in the time of flight for an on-axis particle vs particles injected at 3 mm radius.

Table 4: Variation of Transit Time Due to Path Difference in the First Three 22 Gap Sections

Ion	E_{inj}, MV	U_T, MV	no magnets Δt, ns	with magnets Δt, ns
H^{-1}	0.07	3	0.312	0.312
Ni^{-1}	0.15	14.4	0.120	0.124

Alternative Magnet Positioning and Orientation to Reduce Overall Beam Steering

A proton beam is injected at 150 keV in this simulation at a terminal voltage of 14.3 MV, or 25 kV/gap. The geometry of this simulation is shown in Fig. 5.

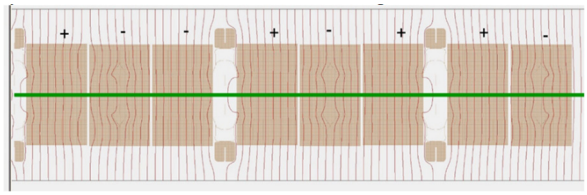

Figure 5: Single plane magnet orientation. Alternative single plane magnet orientation is shown above each plane.

A beam trajectory for single plane magnet orientation, zoomed and enlarged in radial coordinate, is shown in Fig. 6.

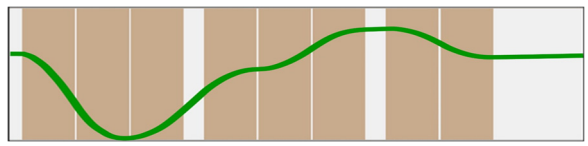

Figure 6. Single plane magnet orientation stretched in the vertical axis to amplify trajectory.

Most importantly, the magnets must still be able to suppress electrons. Here in Fig. 7 we have a distribution of electrons created in a 24 mm diameter cylinder along the length of the tubes covered by magnets. These electrons simulate those created by the beam striking residual gas particles as it travels through the 14UD.

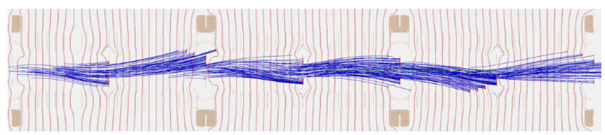

Figure 7: Electron trajectories for single plane magnet orientation.

DISCUSSION

In the LE section tube, the diameter of the ion beam injected is about 5 mm, which is much smaller than the minimum diameter of aperture of 25 mm. Therefore, charge exchange is the dominating process. The charge of the negative ion is not in equilibrium. The stripping of one or a few electrons in one collision can take place with a cross section of the order of 10^{-15} cm^2. In addition, the ionization of the residual gas atom can take place with considerable probability. Secondary electrons and charged particles will travel and gain some energy before they are stopped on the electrodes. They may also cause an additional ionization of residual gas and release more secondary electrons when colliding with the electrodes. In the case of the ANU suppression system based on V-electrodes, the electrons originating on axis are not stopped. One can expect a flux of high energy electrons travelling toward the terminal that are eventually intercepted by an electrode surface facing the top of accelerator as shown in Fig. 1. The discoloration

ISBN: 978-3-95450-240-0 ISSN: 2673-5547 doi:10.18429/JACoW-HIAT2022-MO1C3

of top surface (Fig. 1, 1A) is possibly caused by bombardment of negatively charged particles travelling toward the terminal.

After passing the stripper there is a distribution of charge states but only the selected state is focused properly through the HE section. The same is valid for the HE stripper. The neighbouring charges are over-focused or underfocused with the quadrupole terminal lens. Eventually they are stopped on the electrodes or apertures in the HE tubes producing secondary electrons. One can expect electrons produced on electrodes and in residual gas to travel back to the terminal. Therefore both surfaces of the tube electrodes might be exposed to particle bombardment. The consequences are:

(i) An additional outgassing rate produced by the bombardment of the tube electrodes
(ii) Production of secondary particles which cause additional ionization.

The production of X-ray inside the tube, which ionizes the insulating gas leading to radial loss current between column and tank. This will result in a higher potential difference between electrodes near the terminal causing overvoltage. The feedback character of the process described determines a criticality condition for the maximum injected current.

SIMION simulations confirm that the V electrodes are an efficient suppression option for electrons originating on apertures, Fig. 2. However, this option does not eliminate e- originating on the beam axis in residual gas. SIMION simulations also confirm that the magnets are a universal suppression option for electrons originating on the beam axis and on apertures as shown in Fig. 3 even without using V electrodes. Simulations addressed the suppression of electrons originating on apertures in new NEC 21 or 22 gap tubes. The following conclusions are drawn from the results shown in Table 1.

(i) Poor suppression with flat electrodes and without magnets
(ii) Excellent suppression with flat electrodes (or V electrodes) and B field
(iii) Medium suppression if using V electrodes without B field
(iv On axis electrons generated from the beam interacting with gas are generally not able to be suppressed with V electrodes, however the magnetic field is able to steer them to terminate within a tube.

The main issue with the "spiral" magnetic field is significant steering of the beam both in LE and HE sections, Fig. 4. The analytical model was validated by comparison with SIMION simulations as per Table 2. Then it was applied to calculate beam displacement after passing through LE and HE sections of the 14UD as shown in Table 3. In the LE section the displacement was in excess of 10 mm. In the HE section the maximum displacement of the beam was about 10 mm, but this calculated value is underestimated. The displacement is higher for a beam of low M and at a lower terminal voltage. A high level of steering in both LE and HE sections makes good overall transmission through the entire accelerator impossible. This is specifically important in the case of the ANU 14UD where there is no terminal steering capability. A terminal steerer has to be implemented if "spiral" magnetic suppression is chosen. No significant effect of the magnets on pulsed beam broadening was noticed as per Table 4.

A good alternative to the "spiral" B filed might be a "snake" B field configuration (Fig. 5) in which case the net offset could be negligibly small, see Fig. 6. The net offset in this case is +0.002 mm over 830 mm.

The next set of 8 magnets could be arranged in the opposite direction to try to cancel this net effect. The magnetic suppression is nevertheless not compromised, Fig. 7. The electrons seem to terminate well, mainly at the apertures with an average energy of 290 keV comparable to the 222 keV using the NEC rotated magnet arrangement.

In response to the ANU single plane proposal, NEC suggested using spiral B configuration with half gradients on entry and exit tubes in X and Y directions to compensate. In this case the field configuration would be to put ½ strength magnets on the first and last 20-gap tubes in the first 6 LE units, with, for example, the first 10 gaps in +X, the second 10 gaps in +Y, then full strength 10 gaps −X, 10 gaps −Y, 10 gaps +X, 10 gaps +Y, ..., down to the last tube section with half field 10 gaps −X, and finally 10 gaps -Y. The next eight units after the dead section would follow the same pattern. NEC simulations show that the net deflections in that first 6 units are very small.

CONCLUSION

The preferred technologies for successful implementation of the upgrade of the entire population of 14UD acceleration tubes is based on NEC 20 gap tubes with magnetic electron suppression and minimized steering of ion beam. The minimization of overall steering can be achieved by keeping the integral of B field distribution along beam axis to zero. This option is possible for flat B field distribution ("snake" configuration) or 2D distribution ("spiral" B configuration).

REFERENCES

[1] D.C. Weisser and M.D. Malev, "NEC accelerator tube upgrade: 16.7 MV in a 14UD", *Nucl. Instrum. Meth. Phys. Res., Sect A*, vol. 287 , pp. 64-67, 1990. doi:10.1016/0168-9002(90)91767-6

[2] C.M. Jones, K.A. Erb, D.I. Haynes, J.T. Mitchell, N.F. Ziegler, J.E. Raatz, and R.D. Rathmell, "Tests of compressed geometry acceleration tubes in the Oak Ridge 25URC tandem accelerator", *Nucl. Instrum. Methods Phys. Res., Sect A*, vol. 268, pp. 361-367, 1988. doi:10.1016/0168-9002(88)90536-0

[3] G.A. Norton, "Developments Concerning the NEC High Gradient Accelerating Tube Assemblies", in *Symposium of North Eastern Accelerator Personnel 1987*, Tallahassee, FL, USA, *World Scientific Publishing Company*, pp. 235-245, 1988.

[4] P. Linardakis, N. R. Lobanov, T. B. Tunningley, D. Tsifakis, S. T. Battisson, B. Graham, J. A. Bockwinkel, and J. Heighway, "High Voltage Performance Degradation of the 14UD Tandem Accelerator", *J. Phys.: Conf. Ser.*, vol. 1401, p. 012004, 2020. doi:10.1088/1742-6596/1401/1/012004